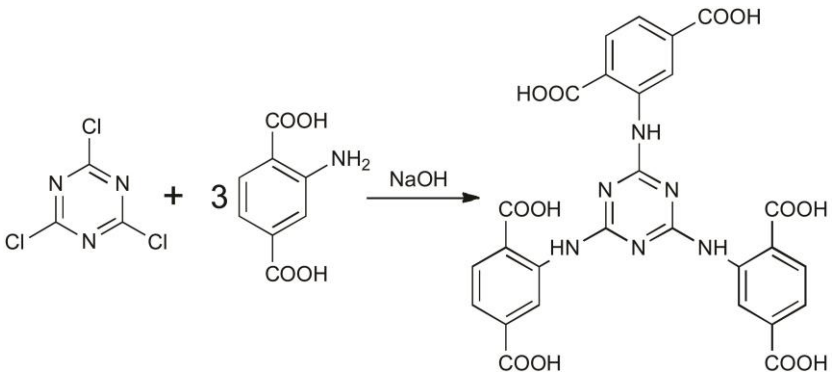

Supplementary Figure S1 Scheme of synthesis of the H_6TATPT ligand.

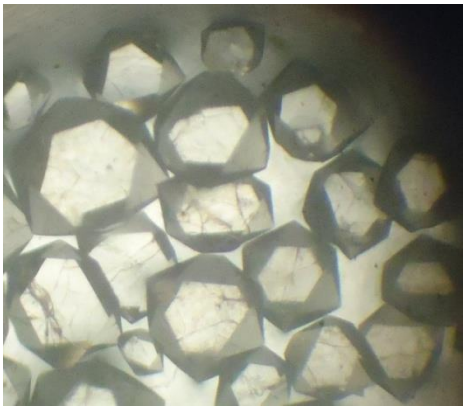

Supplementary Figure S2 Photograph of crystals of compound 1.

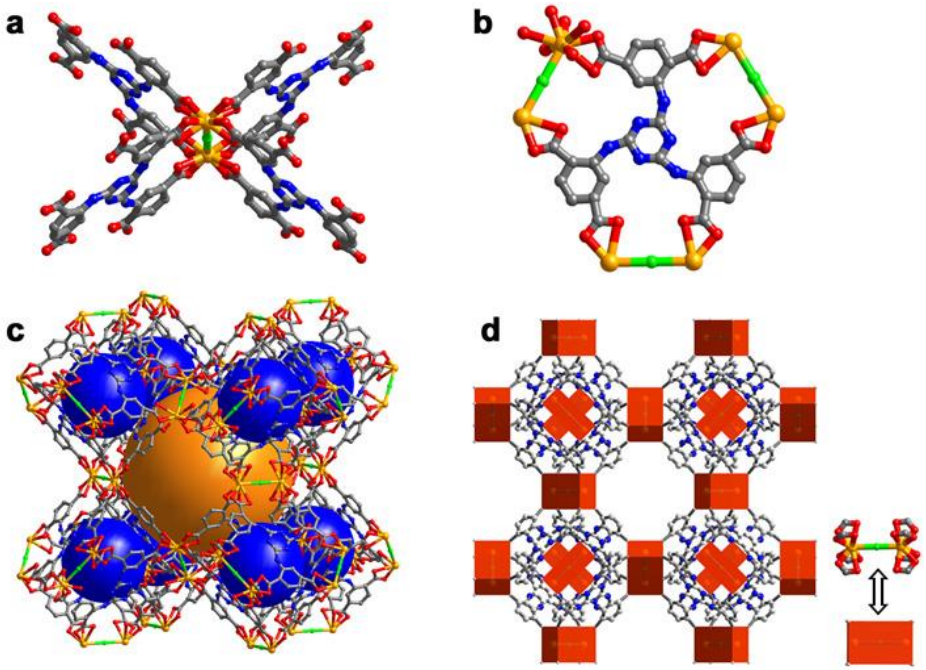

Supplementary Figure S3 Crystal structures of compound 1. (**a**) The coordination environment of Cd^{2+} ion and its connectivity with TATPT ligands, C gray, O red, N blue, Cl green and Cd orange. (**b**) Coordination mode of TATPT ligand. (**c**) Ball and stick representations show the 3D structure in **1** viewed along the *a*-axis. The orange and blue spheres represent the void inside the cages. (**d**) Polyhedral representations of the crystal structure viewed along a axis in which the cuboid represented the $Cd_2(\mu_2\text{-}Cl)(CO_2)_8$ secondary building unit (SBU).

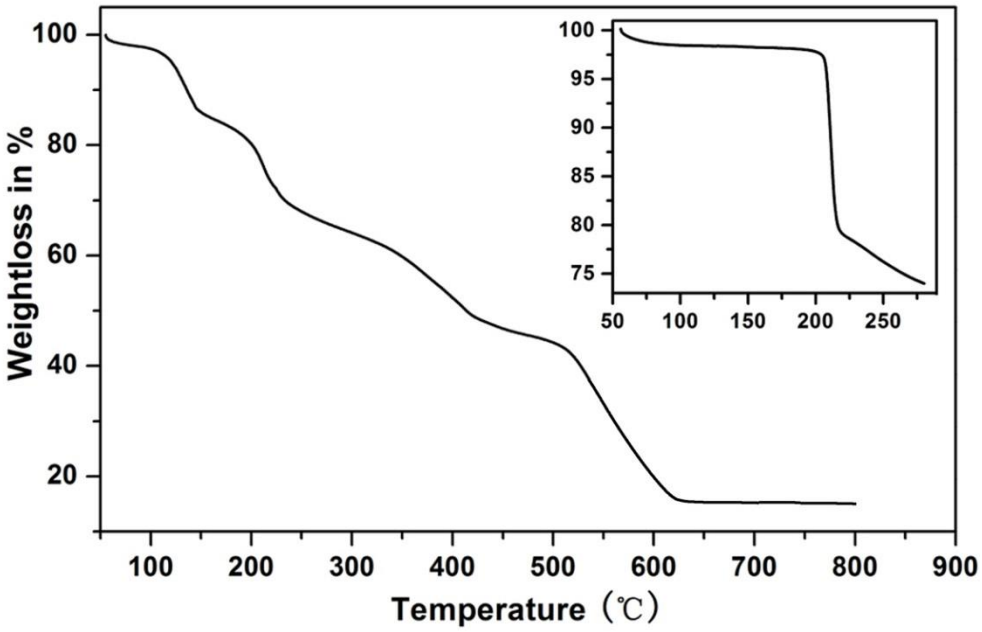

Supplementary Figure S4 TG profile. TG profile of compound **1** under nitrogen gas atmosphere with a heating rate of 10 °C·min^{-1}. The inset is the TG profile of desolvated **1** from 50 to 280 °C under nitrogen gas with a heating rate of 2 °C·min^{-1}.

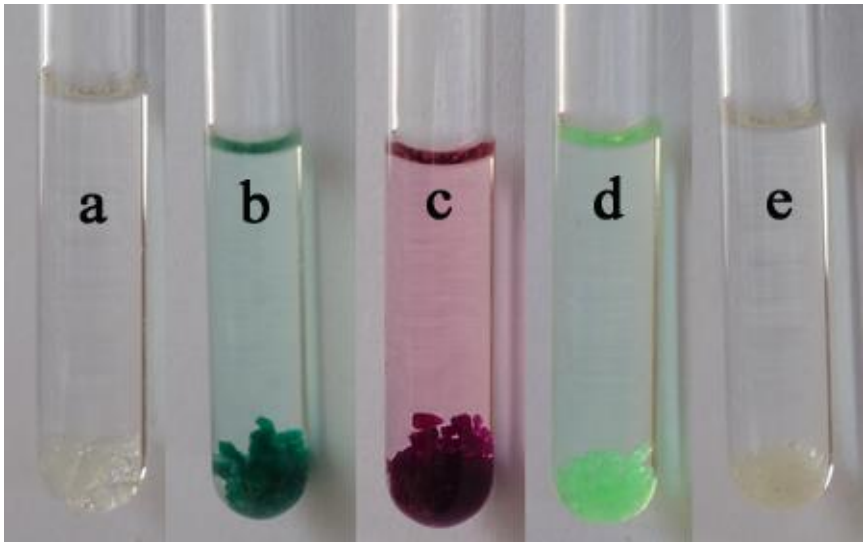

Supplementary Figure S5 Photographs of 1 and samples after ion exchange with transition metals. (**a**) As-synthesized **1**. (**b**) $Cu^{2+}\supset$**1**. (**c**) $Co^{2+}\supset$**1**. (**d**) $Ni^{2+}\supset$**1**. (**e**) $Zn^{2+}\supset$**1**.

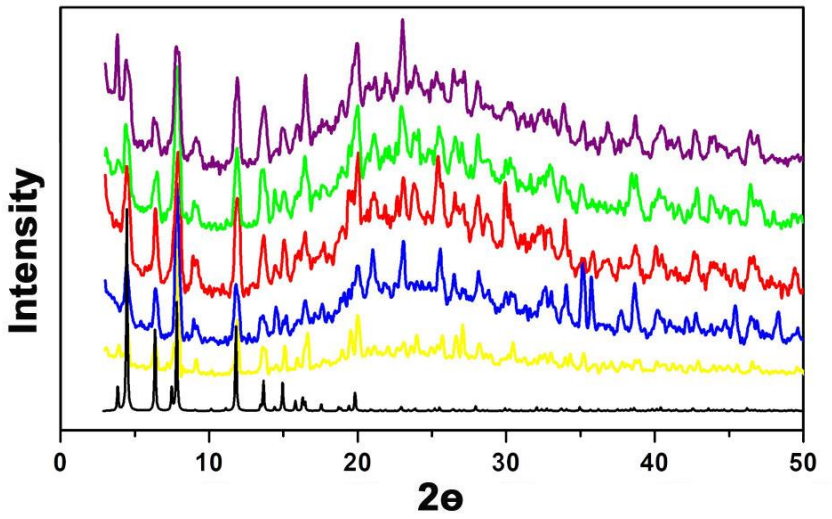

Supplementary Figure S6 PXRD patterns. PXRD patterns for **1** and transition metal ion exchanged **1**. simulated, black; as-synthesized **1**, yellow; $Co^{2+}\supset$**1**, blue; $Ni^{2+}\supset$**1**, red; $Zn^{2+}\supset$**1**, green; $Cu^{2+}\supset$**1**, purple.

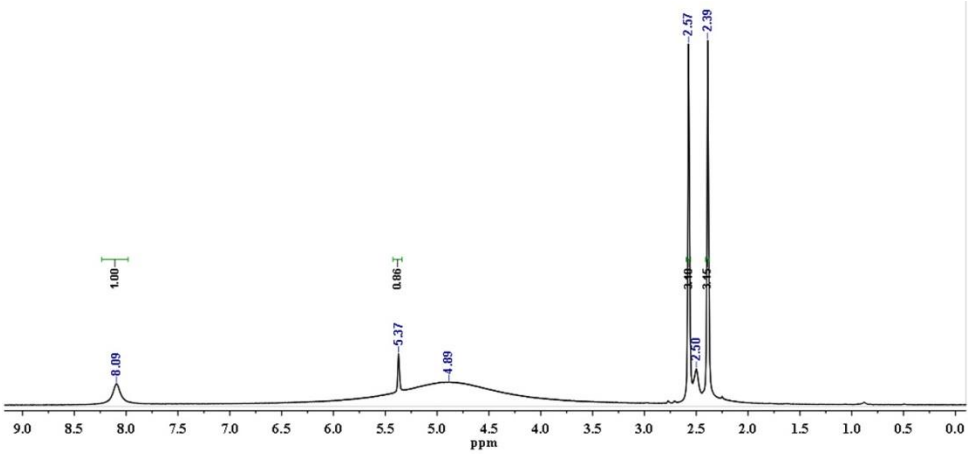

Supplementary Figure S7 ^{1}H NMR spectrum. The ^{1}H NMR spectrum in dmso-$d_6$solution taken after ion exchange experiment.

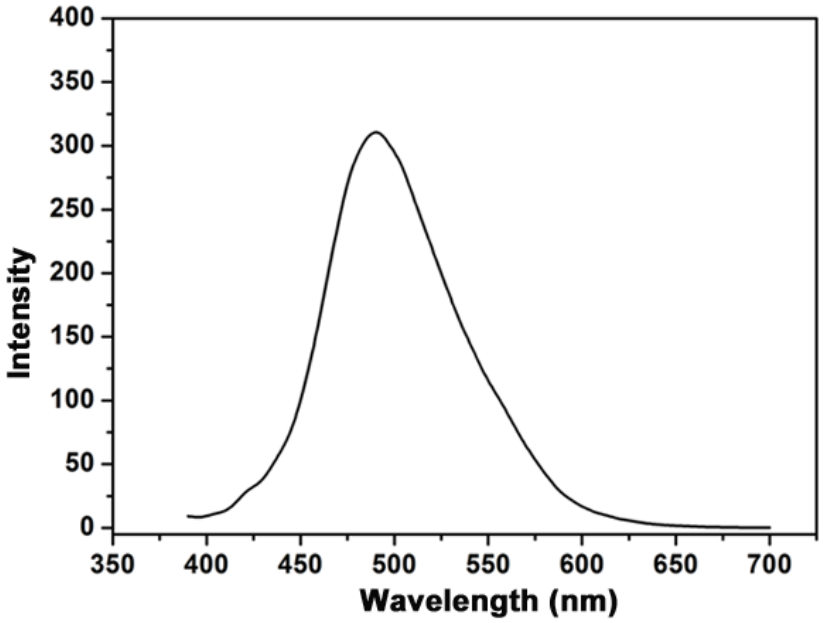

Supplementary Figure S8 photoluminescence spectrum of ligand. Solid photoluminescence spectrum of H_6TATPT ligand at room temperature (λ_{ex} = 370 nm).

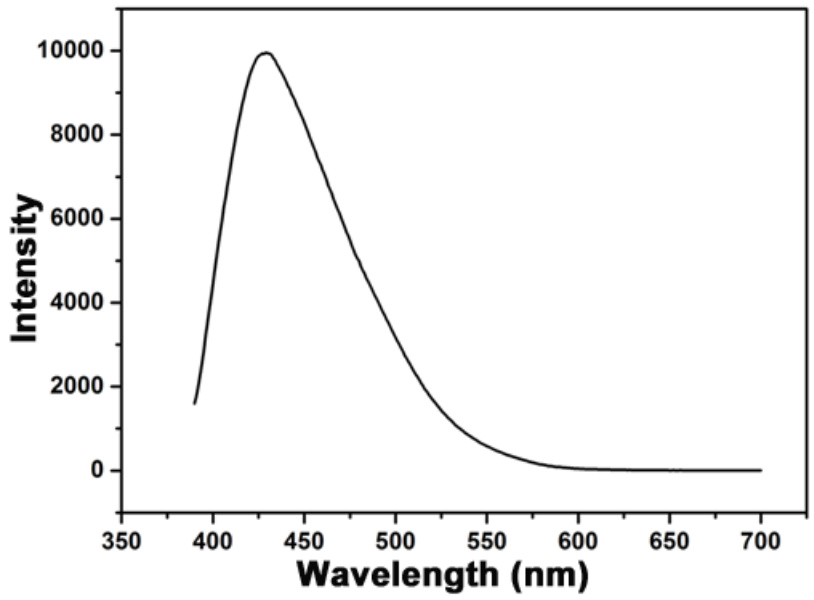

Supplementary Figure S9 photoluminescence spectrum of 1. Solid photoluminescence spectrum of compound **1** at room temperature upon excitation at 370 nm.

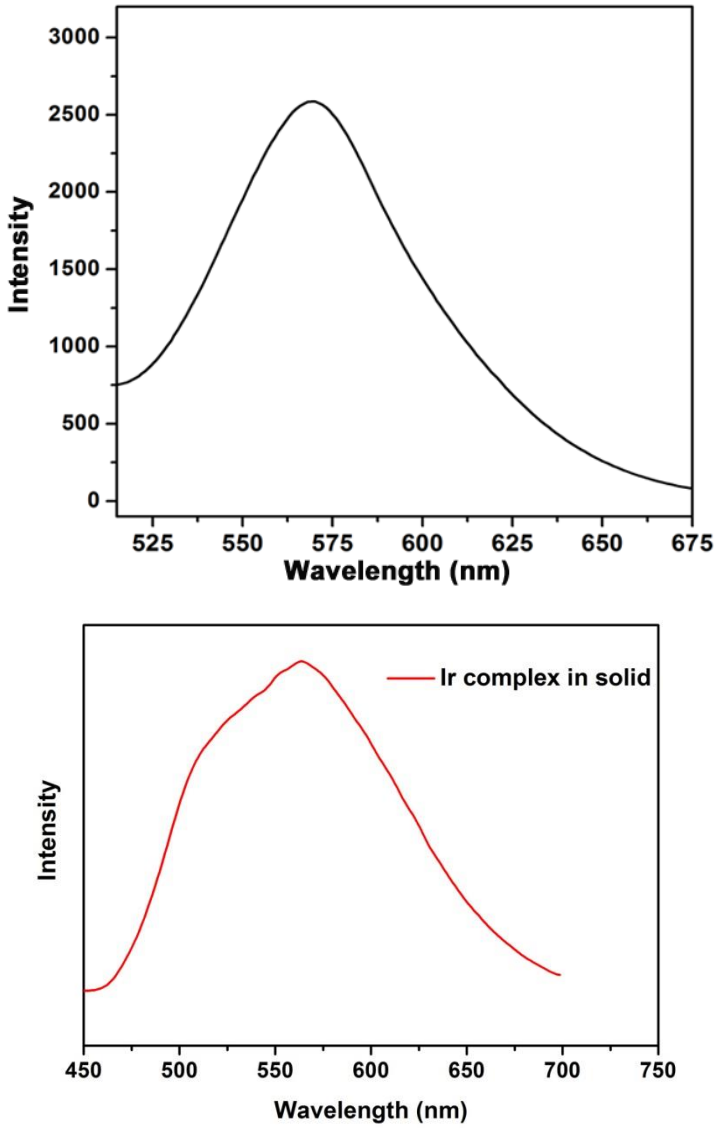

Supplementary Figure S10 photoluminescence spectra of $[Ir(ppy)_2(bpy)][PF_6]$. Room temperature photoluminescence spectra of $[Ir(ppy)_2(bpy)][PF_6]$ in DMF solvent (top) and in solid state (bottom) upon

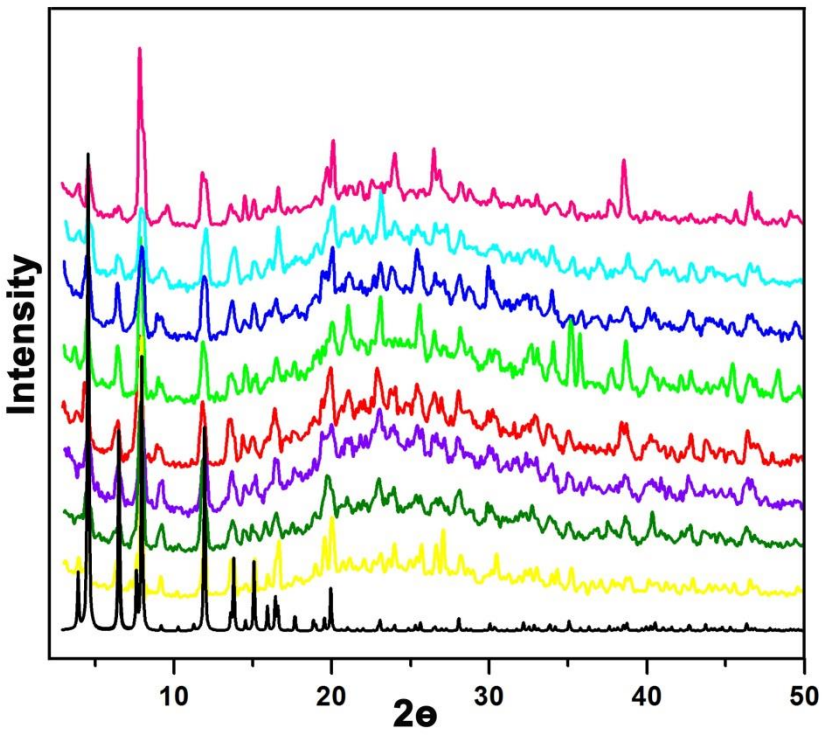

Supplementary Figure S11 PXRD patterns. PXRD patterns for **1** (simulated, black; as-synthesized**1**, yellow) and $[Ir(ppy)_2(bpy)]^+$ encapsulated **1** with different concentrations of $[Ir(ppy)_2(bpy)]^+$ (0.52wt%, olive; 1.04wt%, violet; 3.5wt%, red; 3.7wt%, green; 4.5wt%, blue; 7.5wt%, cyan; 8.8wt% pink).

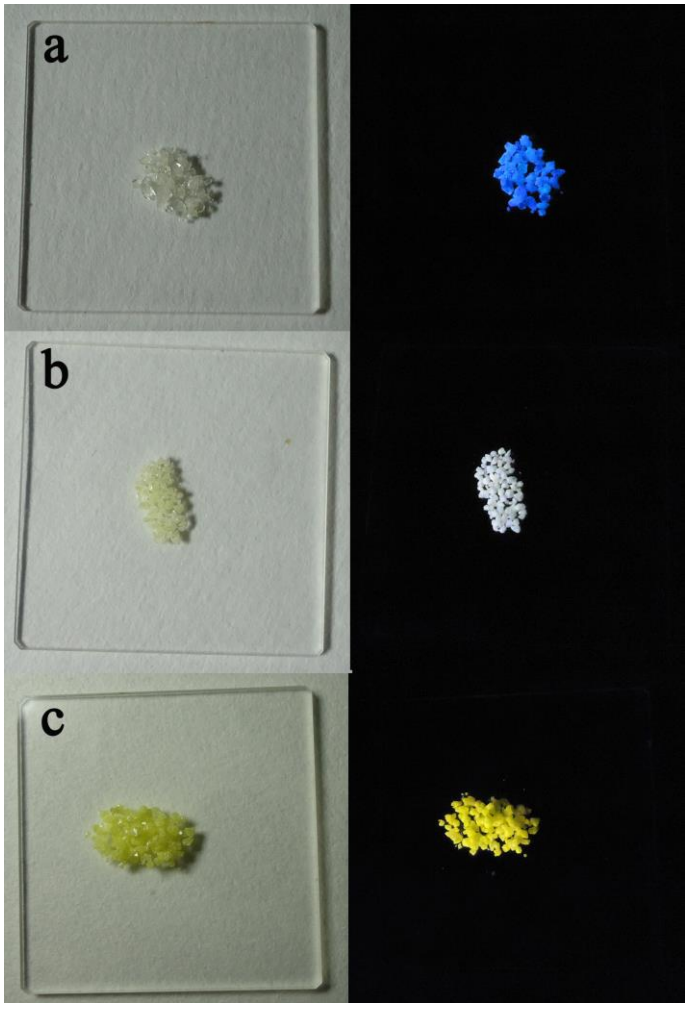

Supplementary Figure S12 Photographs of 1 and $[Ir(ppy)_2(bpy)]^+$@1 (under natural light (left) and laboratory UV light (365 nm, right)). (**a**) As-synthesized **1**. (**b**) 3.5wt% contained $[Ir(ppy)_2(bpy)]^+$@**1**. (**c**) 8.8wt% contained $[Ir(ppy)_2(bpy)]^+$@**1**.

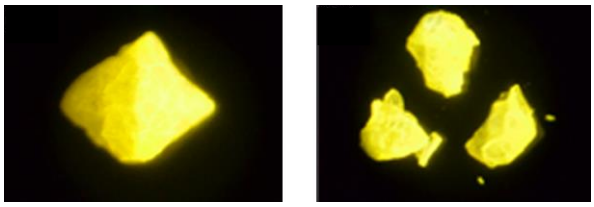

Supplementary Figure S13 Photographs of crystals. Photographs of a single crystal of a freshly grown $[Ir(ppy)_2(bpy)]^+$@**1** (left) and crushed fragments of the same crystal (right).

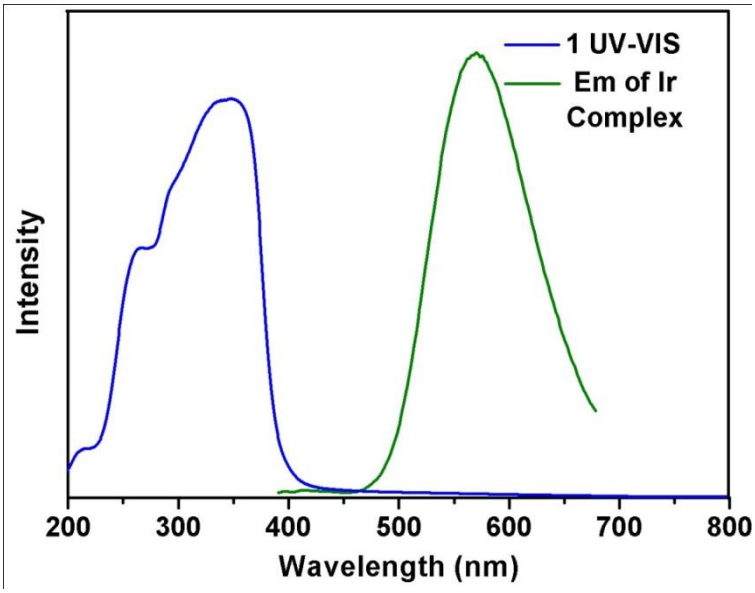

Supplementary Figure S14 Optical spectra. The absorption spectrum of **1** (blue), and emission spectrum of the $[Ir(ppy)_2(bpy)]^+$ complex excited at 370 nm (green).

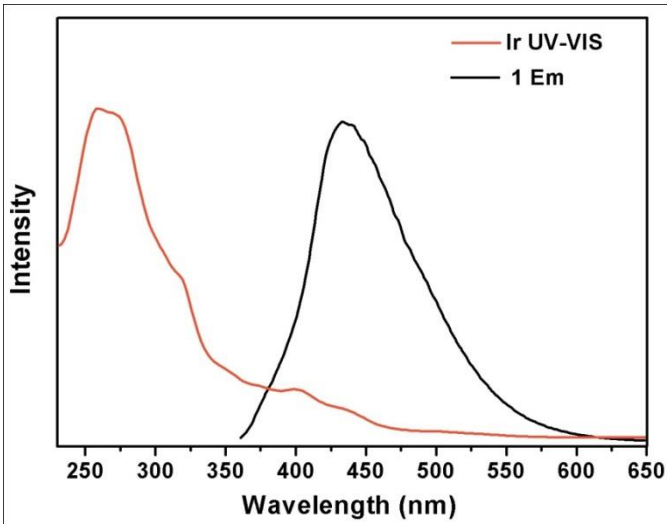

Supplementary Figure S15 Optical spectra. The absorption spectrum of the $[Ir(ppy)_2(bpy)]^+$ complex (red), and emission spectrum of **1** excited at 340 nm (black).

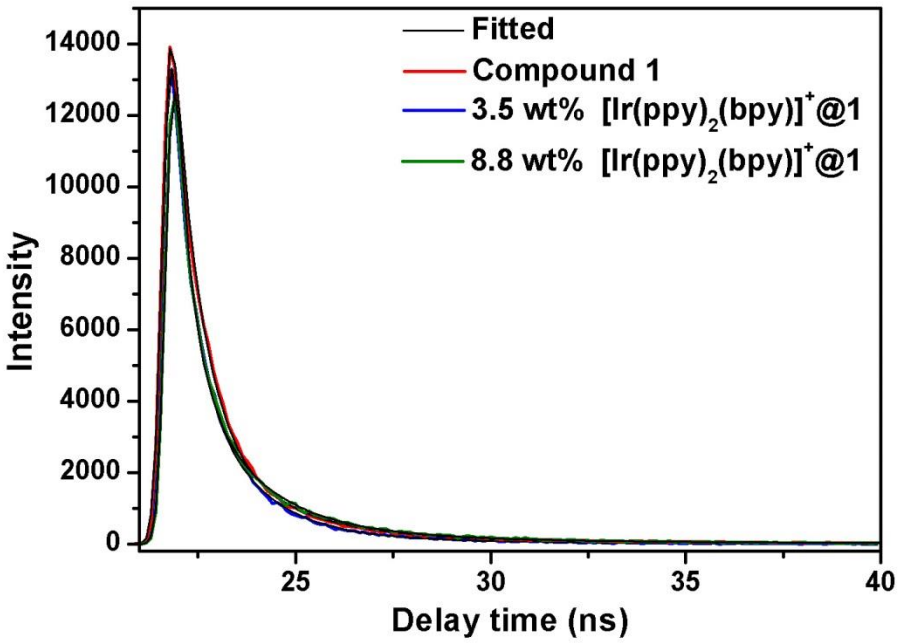

Supplementary Figure S16 Fluorescence decay profiles. Fluorescence decay profiles of **1** and $[Ir(ppy)_2(bpy)]^+$@**1** at λ_{ex} = 370 nm and λ_{em} = 425 nm: black, after fitted; red, compound **1**; blue, 3.5% $[Ir(ppy)_2(bpy)]^+$@**1**; green, 8.8% $[Ir(ppy)_2(bpy)]^+$@**1**.

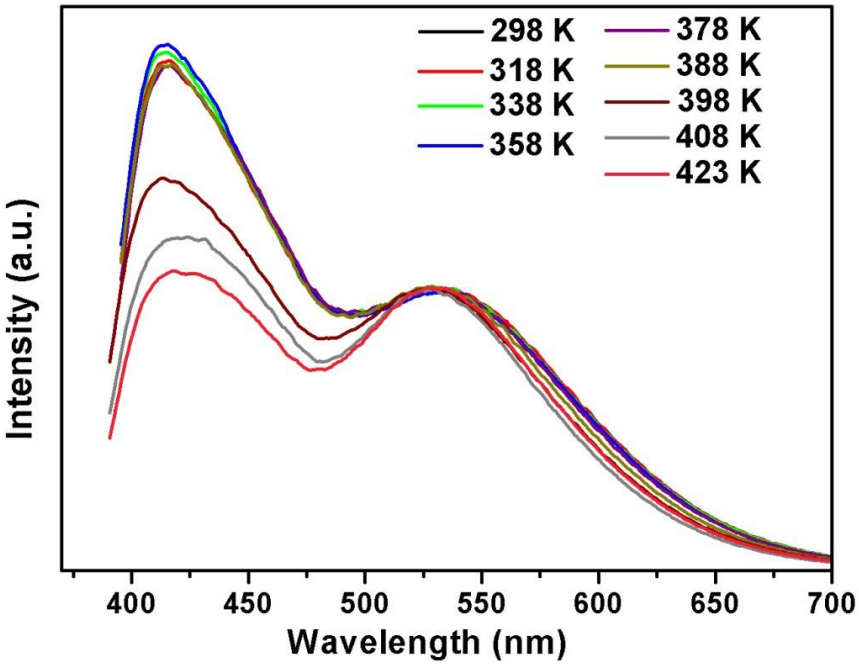

Supplementary Figure S17 Temperature-dependent photoluminescence spectra. Photoluminescence spectra of white-emitting $[Ir(ppy)_2(bpy)]^+$@**1** at different temperatures: black, 298K; red, 318K; green, 338K; blue, 358K; violet, 378K; dark yellow, 388K; wine, 398K; gray, 408K; pink, 423K. All measurements were performed on solid samples at an excitation wavelength λ_{ex} of 370 nm.

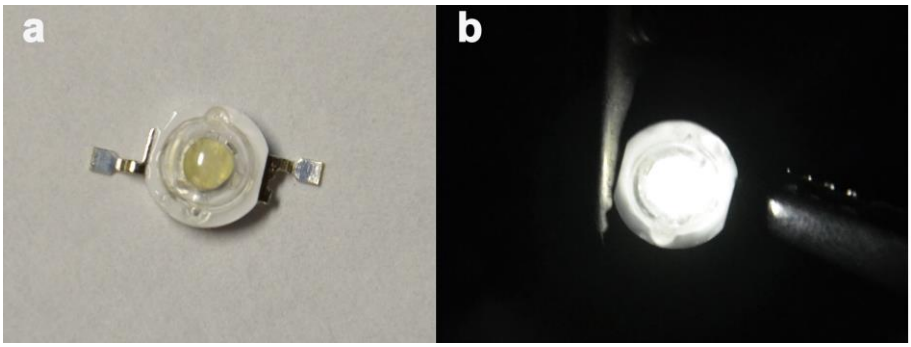

Supplementary Figure S18 Photographs of the white LED fabricated using a UV InGaAsN LED chip and white phosphor of 3.8 wt% $[Ir(ppy)_2(bpy)]^+$@1. (**a**) Without current. (**b**) After applying a forward current of 150 mA.

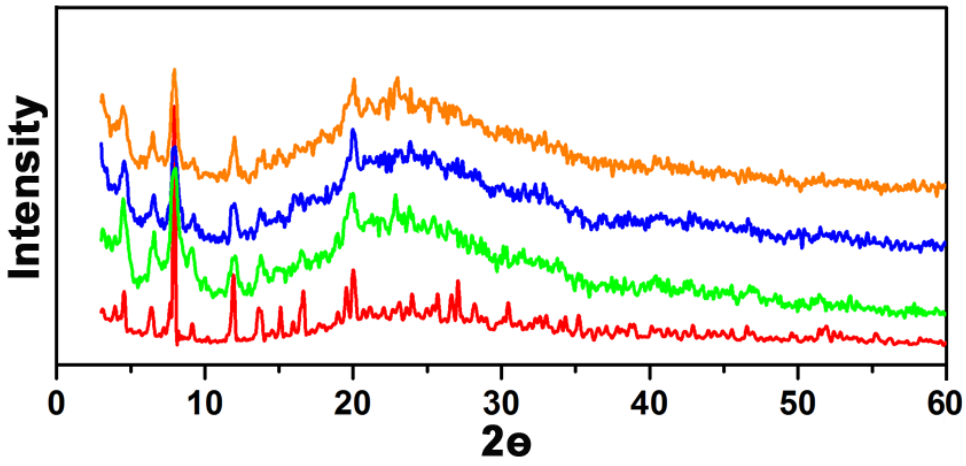

Supplementary Figure S19 PXRD patterns. PXRD patterns for **1** and transition metal exchanged **1**: as-synthesized **1**, red; Eu^{3+}@**1**, green; Tb@**1**, blue; Eu/Tb@**1**, orange.

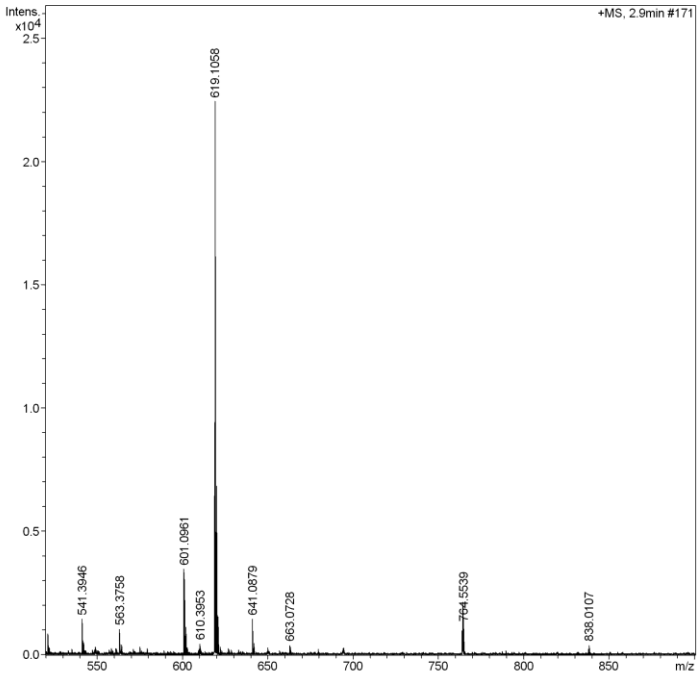

Supplementary Figure S20 HRMS spectrum for the ligand (H_6TATPT). High resolution mass spectra (HRMS) were recorded on Bruck microTof using ESI method. (ESI) *m/z* calcd for $C_{27}H_{18}N_6O_{12}$ $[M+H]^+$: 619.1016 found: 619.1058.

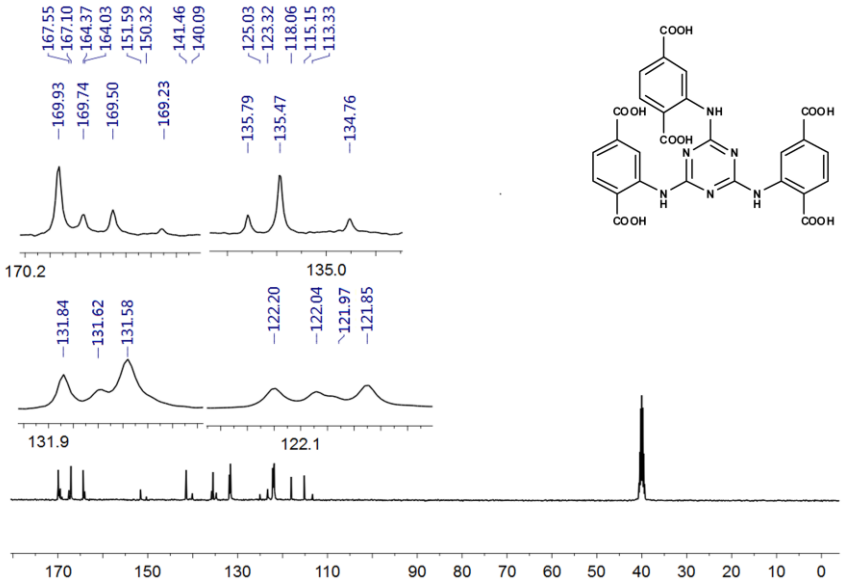

Supplementary Figure S21 ^{13}C-NMR spectrum for the ligand (H_6TATPT, $C_{27}H_{18}N_6O_{12}$). Data were recorded on a Bruker AV400 NMR (400 MHz) at 25 ºC.

Supplementary Table S1 Crystal data and structural refinement of compound **1**; for atomic coordinates, equivalent isotropic displacement parameters, bond lengths, angles, and anisotropic displacement parameters please see the CIF (CCDC code 916964).

Empirical formula	$C_{174}H_{288}N_{51}O_{78}Cl_3Cd_6$
Formula weight	5147.52
Temperature (K)	296
Crystal system	cubic
Space group	*Fm*-3*m*
Unit cell dimensions	
a (Å)	38.527(2)
b (Å)	38.527(2)
c (Å)	38.527(2)
α (°)	90
β (°)	90
γ (°)	90
Volume ($Å^3$)	57186.8 (6)
Z	8
Calculated density (mg/m^3)	1.196
F(000)	12600
Crystal size (mm^3)	0.86 × 0.44 × 0.24
R_{int}	0.0697
Goodness-of-fit on F^2	1.052
Final R indices [I > 2σ(I)]	R_1 = 0.0896, wR_2 = 0.2749

Supplementary Table S2 The concentration of Cu^{2+}, Co^{2+}, Ni^{2+}, and Zn^{2+} in compound **1**.

Transition metal	The concentration of transition metal (wt%)	The concentration of transition metal per formula
Co	5.268	0.37
Cu	7.021	0.46
Ni	3.615	0.26
Zn	4.307	0.28

Supplementary Table S3 The CIE coordinates of $[Ir(ppy)_2(bpy)]^+$@**1** at various concentration of $[Ir(ppy)_2(bpy)]^+$.

Sample	CIE coordinate		The concentration of $[Ir(ppy)_2(bpy)]^+$ (respect to Cd wt%)
	X	Y	
1	0.175	0.145	0
2	0.231	0.206	0.526
3	0.254	0.239	1.04
4	0.311	0.330	3.52
5	0.322	0.352	3.73
6	0.350	0.429	4.52
7	0.371	0.468	7.50
8	0.400	0.501	8.83

Supplementary Table S4 Summary of the quantum yield of the reported white-emitting MOFs.

Compound	Quantum yield	Reference number
PbL2[a]	2−3%	26
Eu-SMOF-1[b]	4.3%	25
ZJU-1:1.5%Tb^{3+}, 2.0%Eu^{3+}[c]	6.8%	12
$[AgL]_n$ nH_2O[d]	10.86%	23
Eu/Tb@**1**[e]	11.3%	this work
$[Ir(ppy)_2(bpy)]^+$@**1**[e]	20.4%	this work

[a]L2 = 2,5-bis(((S)-2-hydroxypropyl)thio)terephthalic acid

[b]SMOF-1 = $In(BTB)_{2/3}(OA)(DEF)_{3/2}$ (BTB = 1,3,5-Tris(4-carboxyphenyl)benzene, OA = oxalic acid, DEF = N,N'-diethylformamide)

[c]ZJU-1 = $Na_3[La(PDA)_3](H_2O)_{12}$ (PDA = pyridine-2,6-dicarboxylate)

[d]L = 4-cyanobenzoate

[e]**1** = $[(CH_3)_2NH_2]_{1.25}[(Cd_{0.5}Cl_{0.25})(TATPT)_{1/3}]\cdot DMF\cdot 1.5H_2O$, (TATPT = 2,4,6-tris(2,5-dicarboxylphenylamino)-1,3,5-triazine, DMF = N,N-Dimethylformamide)

Supplementary Table S5 Quantum yield of white-emitting $[Ir(ppy)_2(bpy)]^+$@**1** at different temperatures.

Temperature (K)	298	378	388	398	408	423
Quantum yield (%)	20.7	21.1	20.1	19.7	18.5	17.9

Supplementary Table S6 Correlated color temperature (CCT) and color rendering index (CRI) for white LED.

CCT (K)	CRI	CIE	
		x	y
5409	84.5	0.30	0.35